Available online at www.sciencedirect.com
SCIENCE DIRECT®
Journal of Power Sources 139 (2005) 96–105
JOURNAL OF POWER SOURCES
www.elsevier.com/locate/jpowsour

Fabrication and preliminary testing of a planar membraneless microchannel fuel cell

Jamie L. Cohen[a], Daron A. Westly[b], Alexander Pechenik[c], Héctor D. Abruña[a,c,*]

[a] *Baker Laboratory, Department of Chemistry and Chemical Biology, Cornell University, Ithaca, NY 14853-1301, USA*
[b] *Cornell Nanoscale Facility, Duffield Hall, Cornell University, Ithaca, NY 14853-1301, USA*
[c] *-92-6, LLC, Ithaca, NY 14850, USA*

Received 1 June 2004; accepted 28 June 2004
Available online 11 September 2004

Abstract

A novel design for a planar membraneless microchannel fuel cell (PM^2FC) as developed by -92-6, LLC is presented. The design, which eliminates the need for a polyelectrolyte membrane (PEM), takes advantage of the laminar flow of fuel and oxidant streams generated at a tapered flow boundary. This gives rise to a "virtual membrane" with diffusion at that interface being the only mode of mass transport between the two solutions. In addition, proton conduction occurs readily, and fuel crossover is virtually eliminated. Our planar design also gives rise to large contact areas between the electrodes and fuel and oxidant streams. As electrodes, we have employed platinum evaporated onto a polyamide film (Kapton®), allowing for the reproducible preparation of large-area electrode surfaces, which are also convenient for testing. Silicon microchannels, of varying width and height, have been tested and parameter optimization has been carried out using formic acid as fuel and oxygen as oxidant. Power densities on the order of 180 $\mu W\,cm^{-2}$ have been obtained using this planar design. The open circuit potentials, as well as the kinetic behavior, observed for the formic acid fuel using this micro-fuel cell are compared to those of macro-fuel cell systems.

Keywords: Membraneless; Planar; Fuel cell; Fabrication

1. Introduction

Recently, there has been much emphasis on the development of novel fuel cell technologies as portable high energy density power sources for consumer electronics, military applications, medical diagnostic equipment, and mobile communication [1]. These systems must be lightweight, energy efficient, and able to operate for long periods of time without refueling. This interest in miniaturization of power sources has been expanded to microsystems for powering MEMs and related devices, such as "lab-on-a-chip" systems and micropumping assemblies [1]. Merging the development of fuel cells with micro-technology has led to the study of microfuel cells and their application to micro-devices, as well as to a myriad of portable systems.

One of the most challenging aspects of the miniaturization of fuel cells is the polymer electrolyte membrane (PEM) [2,3], which suffers from numerous problems including: drying out of the membrane (especially at high operating temperatures), fuel crossover into the oxidizer, in addition to the high expense typically associated with their development. All of these problems are further compounded by the need to decrease the thickness (further increasing the complication of the network structure) of the PEM when designing a micro-fuel cell. Incorporation of a PEM has been achieved in a number of micro-fuel cells studied to date [4–7]. A number of these are biofuel cells [8–10]. Recently, there have also been a number of biofuel cells that employ enzymes as catalysts at both the anode and cathode surfaces in order to achieve some degree of selectivity to the fuel/oxidizer thus decreasing the problem of fuel crossover and eliminating the need for a PEM [11–14]. While these enzymatic redox systems can provide the desired selectivity, they typically generate

* Corresponding author. Tel.: +1 607 255 4720; fax: +1 607 255 9864.
E-mail address: hda1@cornell.edu (H.D. Abruña).

0378-7753/$ – see front matter © 2004 Elsevier B.V. All rights reserved.
doi:10.1016/j.jpowsour.2004.06.072

very low power and suffer from all of the problems attendant to the use of enzymes, with long-term stability being especially problematic. The PEM also takes up much of the space in the non-enzymatic micro-fuel cells being developed, thus limiting the size of the final device. Elimination of the PEM, as well as eliminating the need for enzymatic selectivity, in micro-fuel cell designs will allow the dimensions of the fuel cell to drop well below those already achieved, as well as facilitate fabrication and system integration.

The design presented here not only eliminates the need for a PEM, but also provides a versatile test platform for a planar membraneless microfluidic fuel cell. This system is based on the establishment of laminar flow of fuel and oxidant solution streams separated by a "virtual membrane", which is actually the diffusive interface between the two solutions. This interface allows for proton conductivity, while minimizing mixing of the two solutions. Laminar flow has been used in numerous systems because of the advantages it affords, especially the minimal mixing of solutions flowing side by side. There have been studies for the development of sensors taking advantage of laminar flow, as well as using the diffusive interface for microfabrication of small wires or polymer strands inside microchannels. Moreover, much theoretical work has been done in order to understand the mixing behavior of two solutions flowing in a laminar fashion side by side [15–18].

Currently, laminar flow has been employed in developing micro-fuel cells. Previous work done, as well as very recent work by Choban et al., has demonstrated that laminar flow can be used in order to create a micro-fuel cell with a diffusive interface as the membrane, thus eliminating the need for a PEM [19–21]. Their specific design is based on a Y-shaped microchannel injected with two fuels side by side. Electrodes whose areas were enhanced with nanoparticles of Pt were deposited in a two-step process requiring a complex evaporation step and subsequent electrodeposition step. These electrodes were positioned on the sides of the microchannel to form the anode and cathode, respectively. However, the complicated evaporation techniques necessary, fabrication limitations, as well as the lack of versatility of this micro-fuel cell platform make this design somewhat impractical.

Our planar design has several advantages over previous designs. In particular, it takes advantage of the laminar flow conditions that exist between two large parallel plates with a microscopic separation between them. Specifically, our approach is based on the use of what we term a "tapered flow boundary" (see Fig. 1) designed to establish a condition of laminar flow of two solution streams flowing on either side of the boundary prior to coming into contact. The advantages that accrue when adopting the planar microfluidic configuration over other (e.g. microchannel) configurations include (a) deposition of electrode materials becomes a manageable process based on sputtering and/or evaporation techniques, (b) the large solution/electrode interfacial area available in this design can lead to higher power devices, (c) the stacking of devices can lead to potentially high power systems taking up small volumes, and (d) most processing and manufacturing routines are industrially-scalable and in the future could be carried out using polymer substrates.

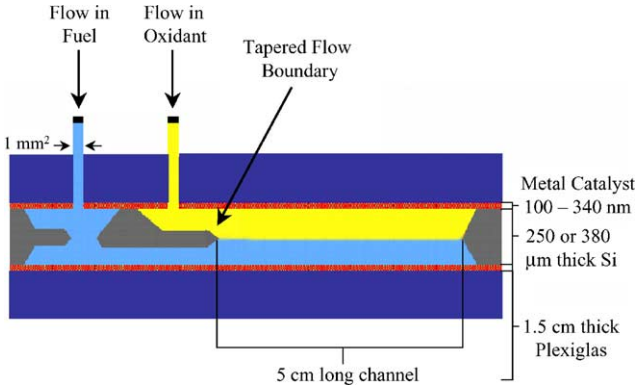

Fig. 1. Side view of the planar microfluidic membraneless micro-fuel cell.

We describe herein the development of such a planar membraneless microchannel fuel cell (PM^2FC) and present preliminary results of its power-producing capabilities.

2. Experimental

2.1. Chemical reagents and instrumentation

Establishment of laminar flow in the silicon microchannels was determined using aqueous solutions of $FeCl_2$ (Sigma–Aldrich, Milwaukee, WI) and bathophenanthroline sulphonate (GFS Chemicals, Powell, OH). Millipore water was used for all aqueous solutions (18 MΩ cm, Millipore Milli-Q). The fuel chosen to test the behavior of the planar micro-fuel cell design was 0.5 M formic acid (Fisher Chemical, 88% Certified ACS, Fairlawn, NJ) in 0.1 M H_2SO_4 (J.T. Baker-Ultrapure Reagent, Phillipsburg, NJ). Fuel solutions were bubbled using N_2 (Airgas Inc.) for 30 min prior to use in the fuel cell. The oxidant was typically 0.1 M H_2SO_4 aerated with O_2 gas (Airgas Inc.) for 30 min prior to introduction into the fuel cell. Bismuth studies were carried out using 0.5 mM Bi_2O_3 (GFS Chemicals, Powell, OH) in 0.1 M H_2SO_4 following the previously documented procedure [22].

All cyclic voltammetry experiments for characterization of the platinum thin film electrodes were carried out using a CV-27 potentiostat (Bioanalytical Systems, West Lafayette, IN). The reference electrode was Ag/AgCl (sat. NaCl) and the counter electrode was a large area Pt wire coil. All electrochemical measurements were carried out in aqueous 0.1 M H_2SO_4 (J.T. Baker-Ultrapure Reagent). Fuel and oxidant were pumped into the PM^2FC using a dual syringe pump (KD Scientific, Holliston, MA) with two syringes (Becton Dikinson lewar-lock 60 cc) affixed with polyethylene tubing (o.d. 2 mm) in order to integrate the pumping system to the PM^2FC. A HeathKit variable load resistor was used in conjunction with a digital multimeter (Keithley, Cleveland, OH) in order to carry out power measurements.

2.2. PM^2FC materials considerations

During the development of the PM^2FC design, numerous materials and processing aspects had to be addressed in order to facilitate the fabrication of a reliable and versatile fuel cell platform. This platform, in turn, served as a testbed for further development of this design. These aspects involved (a) the substrate used for the microchannel design, (b) nature of the electrocatalyst and its deposition method, (c) microstructure of the catalyst, as well as the nature of the substrate onto which the catalyst was deposited, (d) assembly of the electrodes and channel structure into a liquid-tight sealed assembly, as well as (e) interfacing the microchannel device with macro-scale instrumentation and a fluid-delivery system.

Many of the above aspects dealt directly with the parallel-plate electrodes that were employed in the microchannel fuel cell. This fuel cell platform was designed to be versatile and thus accommodate microchannels of varying thickness, length, width, and number in order to have deliberate control over the power output of the cell. The development of a flexible, stable, and reusable electrode using 300 FN Kapton® was important in order to have a reproducible electrode surface that was easily integrated into each of the microchannel designs employed.

Silicon was chosen as the substrate for microchannel development. The photolithographic steps used to process silicon are well established and are well-suited for the fabrication of devices for preliminary characterization. Silicon also provided a rigid substrate that was easy to work with, and yielded channels of reproducible quality. While this fuel cell can be run at room temperature, the silicon substrate will allow the cell to be operated at elevated temperatures in order to enhance fuel oxidation with no change to the fuel cell platform itself. By using basic photolithography for silicon processing, one can take advantage of the ease with which parameters can be varied, and thus optimization of microchannel dimensions can be carried out in relatively short time periods.

The test fuel system for this micro-fuel cell device was formic acid [23,24]. Platinum has been shown to catalyze the oxidation of formic acid and it has been employed during preliminary investigations of the performance of fuel cells.

$$\text{Anode reaction}: \quad \mathrm{HCOOH} \rightarrow 2\mathrm{H^+} + 2\mathrm{e^-} + \mathrm{CO_2}$$

$$E^0 = 0.22\,\mathrm{V}$$

$$\text{Cathode reaction}: \quad 4\mathrm{H^+} + \mathrm{O_2} + 4\mathrm{e^-} \rightarrow 2\mathrm{H_2O}$$

$$E^0 = 1.23\,\mathrm{V}$$

While there are disadvantages when using formic acid, such as CO poisoning of the Pt catalyst, it was a convenient, as well as easily controlled, system with a large open circuit potential and high electrochemical efficiency in order to carry out careful parameter optimization of this initial design [21].

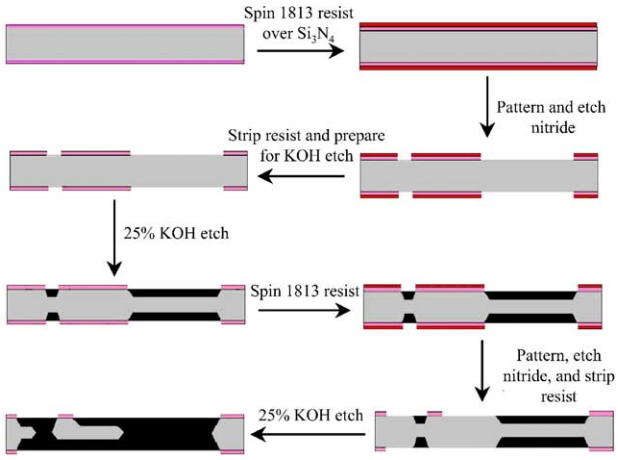

Fig. 2. Process flow for silicon microchannel fabrication.

2.3. Microchannel fabrication

Microchannels were fabricating employing standard photolithography techniques at the Cornell Nanoscale Facility (CNF). Standard 4 in. double-sided polished ⟨1 0 0⟩ silicon wafers (250 μm or 380 μm thick) with 100 nm of Si_3N_4 grown on both sides were used. The process flow is summarized in Fig. 2. L-Edit Pro (Tanner EDA Products) was used to design the CAD for the masks. An optical pattern generator (GCA PG3600F) was used to write the masks, which were 5 $in.^2$ chrome-coated glass. The resist used for processing was Shipley 1813 photoresist (Shipley 1800 Series) spun at 3000 rpm for 60 s. Wafers were then hard baked at 115 °C for 2 min on a vacuum hotplate. A contact aligner (EV 620, Electronic Visions Group) was used to transfer the pattern from the mask to the resist-coated silicon wafers. UV lamp exposure times varied between 6 and 20 s. The wafers were then developed, using Shipley 300 MIF developer, for 60 s and the nitride layer was etched using CF_4 chemistry in an RIE system (Oxford Plasma Lab 80 + RIE System, Oxford Instruments). After repeating these steps for the backside of the wafer, the resist was stripped with acetone and the wafers were put into a 25% KOH solution held at 90 °C in order to etch the silicon at a rate of about 2 μm/min. The 380 μm wafers were etched for approx. 1 h or until 80 μm of silicon on each side of the wafer were etched. For the 250 μm wafers, this etch time was reduced in order to etch approx. 60 μm on each side of the wafer. This etch defined the thickness of the tapered flow boundary. Two subsequent patterning and nitride etch cycles were carried out in order to pattern the tapered flow boundary. The wafers were then soaked in hot Nanostrip (Cyantek Corp., Fremont, CA) at 90 °C for 10 min, and a second 25% KOH etch was carried out at 90 °C. The second KOH etch shaped a tapered flow boundary of approximately 120–180 μm thick, which was thinned down to a thickness of the order of less than 100 μm. The tapered edge at the end formed due to the selectivity of the KOH etch to the ⟨1 0 0⟩ and ⟨1 1 0⟩ planes of the silicon, thus cre-

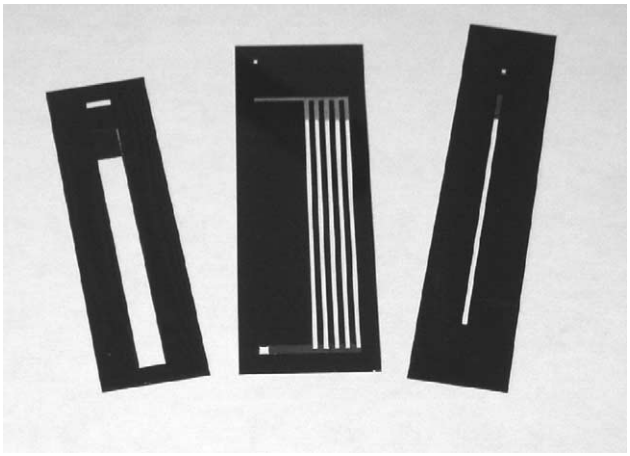

Fig. 3. From left to right: 5 mm wide, 5 cm long microchannel 250 μm thick, a 5-microchannel array of 1 mm wide and 5 cm long microchannels, 380 μm thick, and a 1 mm wide, 5 cm long microchannel, 380 μm thick.

ating an angle of 54.7° relative to the surface normal. The sections of the channel, which were etched previously, continued to be etched until all of the silicon was removed. The final microchannels were then coated with a 1 μm layer of Parylene-C (Labcoater) in order to electrically isolate the silicon channel from the electrodes and electrical contacts, as well as to facilitate a watertight seal in the final device.

Using the basic method outlined above, we fabricated the following microchannels, three of which are shown in Fig. 3:

(a) single, 1 and 3 mm wide, 5 cm long, and 380 μm thick microchannels,
(b) single, 1 and 5 mm wide, 5 cm long, and 250 μm thick microchannels,
(c) five-microchannel arrays of 1 mm wide, 5 cm long, and 380 μm thick microchannels in parallel and fed fuel and oxidant simultaneously, and lastly,
(d) stackable single 1 mm wide, 5 cm long, and 380 μm thick microchannels.

2.4. Electrode fabrication

Platinum was chosen for the preliminary investigation of the planar design, as well as parameter optimization, since its behavior, though not ideal/optimal, is well established and thus serves as a reference point for further experimentation. Electron-beam evaporation techniques were employed for the deposition of platinum thin films with various adhesion layers (CVC SC4500 Combination Thermal/E-gun Evaporation System). Preliminary studies were carried out using glass, Kapton® (Dupont, Wilmington, DE) with and without a Teflon overcoating, polypropylene and Tefzel® (a tetrafluoroethylene/ethylene copolymer, DuPont) as substrate materials. In these studies, the adhesion and stability of the deposited film, as well as its electrochemical behavior, were investigated in detail using cyclic voltammetry. In this context, the use of platinum was, again, most convenient since the voltammetric response of polycrystalline platinum is very well established and allows for the determination of the microscopic area of the deposit via the coulometric charge associated with hydrogen adsorption.

Cyclic voltammetry was carried out in 0.1 M H_2SO_4 for platinum film electrodes with varying thickness (between 10 and 100 nm) deposited onto Kapton®, glass, and Tefzel®. Metal adhesion layers were also employed and consisted of either Ti or Ta (between 10 and 50 nm thick). Fig. 4 shows a typical cyclic voltammogram of polycrystalline Pt on a Kapton® substrate. The electrochemical response obtained from the films was that typical of a polycrystalline platinum electrode, and from the hydrogen adsorption charge, roughness factors of ca. 30–50%, depending on the substrate, were determined. That is, the microscopic area was 30–50% larger than the geometric area. These voltammetric experiments indicated that the best substrate for the electrodes was the flexible Teflon-coated 300 FN Kapton®. This was due to the electrode stability and good adhesion of the platinum to this substrate in 0.1 M H_2SO_4, a common electrolyte in fuel cell systems. Kapton® has a variety of attractive characteristics, including its flexibility, chemical inertness, ability to bond to substrates (such as glass and silicon) at reasonable temperatures (ca. 300 °C), as well as the capacity for surface roughening using diamond paste or sandpaper. The platinum film deposited on Kapton® could also be electrochemically roughened, in order to increase the Pt surface area, following the procedure carried described by Bommarito et al. [25].

Finally, one of the greatest advantages of using a flexible polyamide, such as FN Kapton®, as the electrode substrate is the convenience of being able to evaporate platinum onto large sheets and subsequently cutting the electrodes from them. The ability to fabricate multiple electrodes, which are reusable, in a single batch enables rapid characterization of

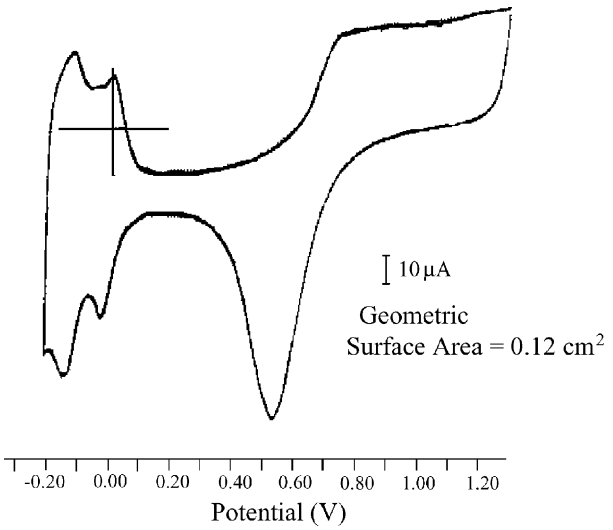

Fig. 4. Cyclic voltammogram of Kapton® with 10 nm of Ta (as an adhesion layer) and 100 nm of Pt evaporated on to the surface in 0.1 M H_2SO_4. Ag/AgCl was used as a reference electrode and a large area Pt wire coil was used as the counter electrode. Scan rate = 0.100 V s^{-1}.

the electrodes and allowed the main focus of optimization and characterization to be on the microchannel design parameters and electrode surface modification for the final working PM^2FC device, without having to worry about tedious processing of the electrodes themselves. Bulk sheets composed of thin films with the following evaporation ratios were fabricated: 20 nm of Ta and 30 nm of Pt, 50 nm of Ta and 50 nm of Pt, as well as 200 nm of Cr, 40 nm of Ta to cap the Cr layer, and 100 nm of Pt, all on 300 FN Kapton®. These electrodes proved to be the most robust under the acidic conditions of the micro-fuel cell, as well as reusable for subsequent experiments.

3. Results and discussion

3.1. Determination of laminar flow

In order to confirm the establishment of laminar flow, aqueous solutions of 1.5 mM $FeCl_2$ and 3.0 mM bathophenanthroline sulphonate (BPS), respectively, were injected into the microchannel by means of a dual syringe pump. Individually, both of these solutions are colorless. However, Fe^{2+} has a very high affinity, and rapid kinetics, for the formation of the tris-chelate of BPS $[Fe(BPS)_3]^{4-}$; which is intensely colored (cherry-red). Fig. 5 shows a planar microchannel into which millimolar solutions of Fe^{2+} and BPS are being fed. As is immediately evident, there is no coloration of the channel area where the two solutions come into contact. The waste solution tube shows the intense coloration of the chelate formed when the two solutions mix as they are transported out of the flow system. This conclusively demonstrates that the solutions have not mixed in the time scale involved in traversing the 5 cm long channel (i.e., for a pumping speed of 0.5 ml min^{-1}, the solution travels at a rate of 4.4 cm s^{-1} in a 380 μm thick channel).

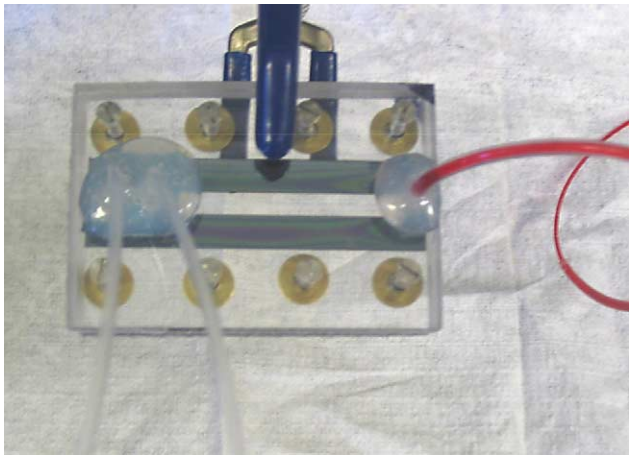

Fig. 5. A 5 mm wide, 5 cm long, and 380 μm thick Si microchannel with Fe^{2+} and BPS flowing. Note the colorless input tubes and microchannel. The cherry-red complex formed when the two solutions are mixed can be seen in the waste tube flowing out of the cell. (For interpretation of the references to color in this figure legend, the reader is referred to the web version of the article.)

3.2. Fuel-cell platform assembly

After establishing that the proposed planar design will indeed generate laminar flow inside the microchannels, fabricated microchannels and electrodes were integrated into a platform that would afford deliberate control over system parameters while design optimization was carried out. Using a clamping assembly system (Fig. 6), the silicon microchannels

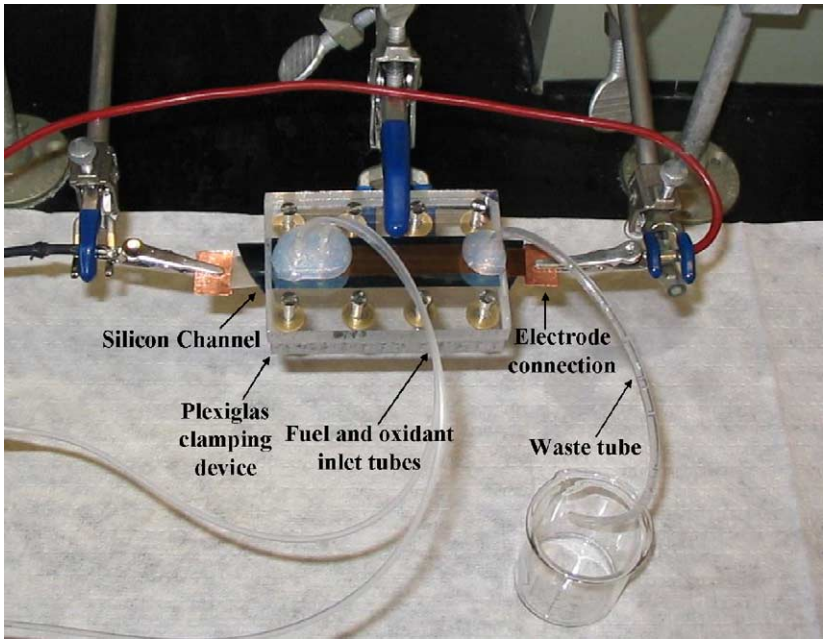

Fig. 6. Clamping system employed as the micro-fuel cell test platform.

were aligned in a Plexiglas cell with Kapton®-based platinum electrodes placed on the top and bottom of the microchannel. The channel and electrodes were then pressed between two Plexiglas plates with eight bolts to apply even pressure along the periphery of the channel, thus creating a watertight cell. The top Plexiglas plate had holes drilled through where fluid interconnects were affixed with epoxy. Holes were cut into the top electrode allowing fluid to pass into the channel and between the anode and cathode. Electrical contact to the electrodes was achieved by allowing their ends to protrude from the device and a copper foil was employed to decrease the contact resistance. The device was connected in series to a variable load resistor and a digital multimeter was used to measure the voltage across the cell when a load was applied. This assembly allowed facile disassembly of the device, which was very important in the early stages of device design optimization. Rapid interchange of electrodes led to fast characterization of various Kapton®-based electrodes, the ability to study surface-modified electrode substrates with ease, as well as the ability to replace an electrode when damaged. The assembly also allowed ready interchange of silicon microchannels. The fabricated microchannels of different dimensions described previously were used to study the ability to modulate power generation, test the reproducibility of the fabrication processes, and determine the ease with which the platform could be reconfigured in order to control the power generated from the fuel cell.

3.3. Formic acid as a test system for the planar micro-fuel cell

Using the platform described in detail above, formic acid and O_2 saturated 0.1 M H_2SO_4 were used as fuel and oxidant, respectively, in order to test the performance of the micro-fuel cell. These data were obtained using 300 FN Kapton® electrodes with deposition ratios noted in the figure captions. The same clamping device was used for all microchannel sizes, excluding the 5-microchannel array, which used a slightly larger clamp due to its larger width.

The fuel and oxidant were fed into the microchannel at flow rates of 0.5 ml min^{-1} in the case of 1 mm wide microchannels, 2 ml min^{-1} for 3 mm wide channels, 2.5 ml min^{-1} for 5 mm wide channels and 5-microchannel arrays, and 1 ml min^{-1} for the stack of two 1 mm wide channels. These flow rates were optimized through a variety of test runs using the device and using the criteria of maximum power production with no leakage of the cell, as well as no introduction of turbulent flow to the system.

Typically, the fuel used was 0.5 M formic acid in 0.1 M H_2SO_4 degassed with N_2 for 30 min and the oxidizer was an O_2 saturated solution of 0.1 M H_2SO_4. The fuel was degassed with N_2 in order to eliminate any O_2 that might be present at the anode and subsequently reduced, which would act as an internal "short circuit" for the device. Initially, however, the oxidizer was air saturated 0.1 M H_2SO_4 with no deliberately added O_2. This generated power densities on the order of only

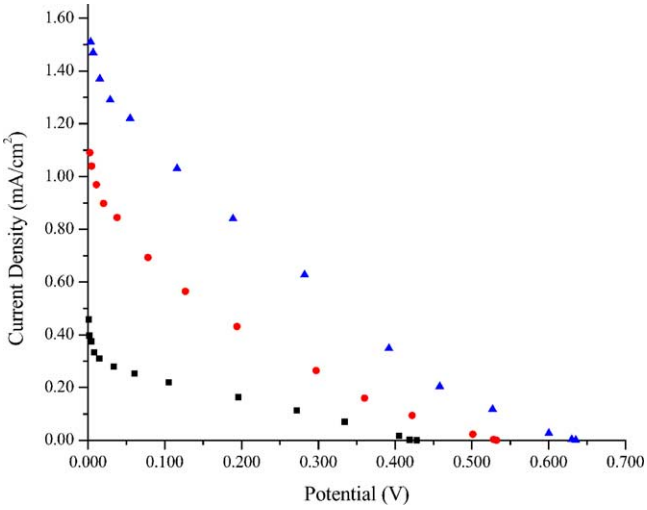

Fig. 7. *I–V* curves for a single 380 μm thick, 5 cm long, and 1 mm wide Si microchannel fuel cell. Kapton® electrodes with 50 nm of Ta and 50 nm of Pt were used. Fuel was 0.5 M formic acid in 0.1 M H_2SO_4 (black squares) bubbled with N_2 (red circles and blue triangles). Oxidant was air saturated 0.1 M H_2SO_4 (black squares) with deliberate addition of O_2 (red circles and blue triangles). Bi-modified Pt anode from immersion in an aqueous solution of 0.5 mM Bi_2O_3 in 0.1 M H_2SO_4 for 2 min (blue triangles). Flow rate = 0.5 ml min^{-1}.

30 μW cm^{-2}. Thus, it was determined that enhancement of the power output of the system could be achieved by simply increasing the O_2 concentration of the oxidant. The oxidant solution was aerated with O_2 gas for 30 min prior to introduction into the micro-fuel cell. All subsequent experiments were carried out with aerated solutions.

3.3.1. Power characteristics for single 1 mm wide microchannels

Fig. 7 shows the *I–V* curves for a 1 mm wide, 380 mm thick microchannel using fuel and oxidizer that were not bubbled (black squares), and that were bubbled using N_2 and O_2 (red circles) for the fuel and oxidant streams, respectively. From the shape of the *I–V* curve, as well as the fact that power density was independent of flow rate, it was determined that the formic acid system is kinetically, and not mass transport, limited. Also, one can qualitatively ascertain the improvements made when using O_2 and N_2 saturated oxidant and fuel, respectively. The improvements are clearly evident in an increase in the open circuit potential of over 100 mV and a current density that more than doubles at zero applied load.

Fig. 8 shows power results obtained with a 380 μm thick microchannel. This is a 1 mm wide channel that is 5 cm in length, thus giving a geometric area of 0.5 cm^2. Current and power densities were determined using the geometric area of the electrodes. The power densities, current densities at zero load, and open circuit potentials obtained for a number of channels are summarized in Table 1. The power generated from a single microchannel device was 86 μW cm^{-2} and the open circuit potential was 0.428 V. The large overpotential required for O_2 reduction, as well as the slow oxidation kinet-

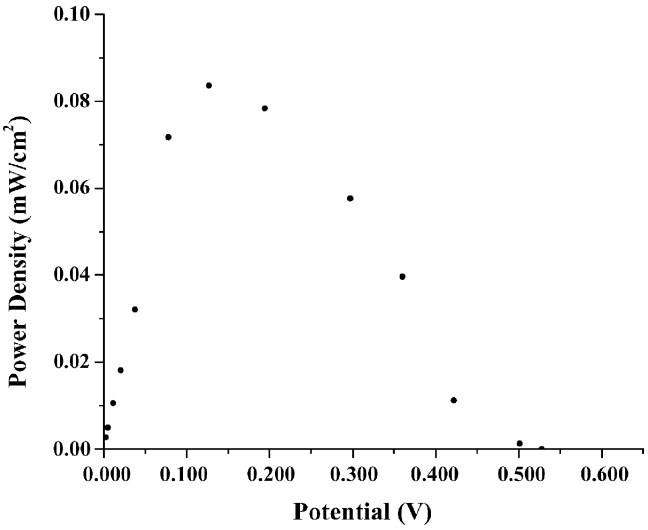

Fig. 8. Power curve for a single 380 μm thick Si microchannel fuel cell. Kapton® electrodes with 50 nm of Ta and 100 nm of Pt were used. Fuel was 0.5 M formic acid in 0.1 M H_2SO_4 bubbled with N_2, oxidizer was 0.1 M H_2SO_4 aerated with O_2, flow rate = 0.5 ml min^{-1}.

ics for formic acid oxidation, account, at least in part, for the open circuit potentials observed. Results similar to those in Fig. 8 were obtained for microchannels 250 μm thick, 1 mm wide, and 5 cm long. When looking at the two channel thicknesses employed, it can be stated that the thickness of the microchannel, in the case of the formic acid system, does not have an effect on the current and power densities. Other fuel systems may show different results and, thus, further investigations will be carried out. In the formic acid case, if power generation is invariant with channel depth, then thinner channels will mean a more compact micro-fuel cell when stacking the individual channels, as well as a decrease in fuel consumption, without loss of power.

3.3.2. Anode surface modification

It is well known that modification of electrode surfaces can dramatically enhance electrocatalytic activity. For example, it has been previously established that the electrocatalytic activity of platinum surfaces towards formic acid oxidation can be greatly enhanced by the adsorption of Bi, As, and Sb [22,26,27]. For example, Bi adsorbed on Pt catalyzes the oxidation of formic acid, as well as ethanol, and decreases CO poisoning of the Pt anode surface. Adatoms of Bi have been found to block sites that are commonly poisoned by CO, to enhance the complete oxidation of small molecule fuels due to electronic effects at the Pt surface, as well as have an affinity for oxygen. This oxygen affinity will become more relevant when we begin to look at other potential small molecule organic fuels, such as methanol and ethanol, which require oxygen to generate CO_2. Surface modification of the anode electrode was carried out using adsorbed Bi adatoms [22], Briefly, adsorption of Bi was carried out by immersing the Pt surface, in our case the Pt anode of our micro-fuel cell, into a 0.5 mM Bi_2O_3 in 0.1 M H_2SO_4 solution for 2–4 min and then rinsing with water. The blue triangles in Fig. 7 show results obtained for a micro-fuel cell with Bi adsorbed onto the electrode surface and pure O_2 dissolved in the oxidizer solution. By adsorbing Bi adatoms onto the surface of the Pt anode, we were able to increase the initial current densities, the open circuit potential, and the power density when employing a single 380 μm thick microchannel with formic acid as the fuel. The initial current densities were increased to over 1.5 mA cm^{-2} and did not drop off dramatically with time due to surface poisoning as was commonly encountered when using bare platinum surfaces. It is also important to note the dramatic increase of 200 mV in the open circuit potential. Power densities obtained were enhanced by nearly 50% when compared to results using unmodified platinum surfaces.

3.3.3. Multiple channel arrays

In order to increase the power obtained from a single device, an array of microchannels was fabricated. Five microchannels, each 380 μm thick, 1 mm wide, and approximately 5 cm long were arranged in parallel and fed simultaneously from the same inlet holes. The waste fuel was removed from the channels by two outlet holes at the end of the channels. A new Plexiglas clamp was made to accommodate the microchannel array and larger electrodes were used in the device. Because the power should scale linearly with area, one would anticipate that there should be five times the power output from this new array when compared to a 1 mm wide single microchannel. Fig. 9 shows the results obtained with

Table 1
Performance of MCFC with formic acid as a test fuel

Channel width[a]	Current at zero load	Open circuit potential (V)	Power
1 mm wide[b]	0.458 mA cm^{-2}	0.428	32 μW cm^{-2}
1 mm wide	1.09 mA cm^{-2}	0.532	86 μW cm^{-2}
1 mm–250 μm thick	0.88 mA cm^{-2}	0.473	85 μW cm^{-2}
1 mm—anode modified with Bi adatoms	1.51 mA cm^{-2}	0.636	180 μW cm^{-2}
Stack of two 1 mm channels	1.16 mA	0.589	118 μW
3 mm	1.4 mA	0.591	160 μW
5 mm–250 μm thick	3.2 mA	0.573	325 μW
5-Microchannel array	2.06 mA	0.641	350 μW
5-Microchannel array—anode modified with Bi adatoms	2.6 mA	0.728	400 μW

[a] All thicknesses 380 μm and lengths 5 cm unless otherwise noted.
[b] Oxidant not deliberately saturated with O_2.

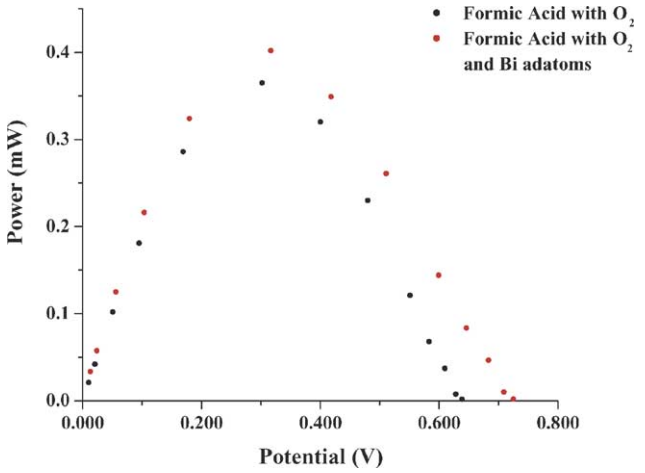

Fig. 9. Power results for a Si 5-microchannel (each l mm wide) array fuel cell. Kapton® electrodes with 50 nm of Ta and 50 nm of Pt were used. Fuel was 0.5 M formic acid in 0.1 M H_2SO_4 bubbled with N_2, oxidizer was 0.1 M H_2SO_4 aerated with O_2, flow rate = 2.5 ml min^{-1}.

the 5-microchannel array with formic acid as the fuel (black circles). The power obtained was 350 μW for a single device. The power generated by this device was larger than anticipated, which can be explained by the electrode surface roughness variations between different electrode evaporations, as well as refinements made throughout the device optimization process. Fig. 9 also shows results for a 5-microchannel array with the anode modified with Bi adatoms (red circles). The power generated was 400 μW and the open circuit potential was over 700 mV. These results do scale linearly with those obtained for a single 1 mm wide microchannel surface-modified with Bi. The results obtained for the multiple channel arrays indicate that the arrays were filling completely and uniformly with no air bubbles preventing laminar flow. Air bubbles trapped in one or more of the microchannels can disrupt the flow of the fuel and oxidant streams, causing a dramatic decrease in the power production of these devices and, as a result, the power output would not scale linearly when compared to single channel devices. Also, the power obtained from the device can be easily controlled due to the linearity with which power generation scales. The versatile planar design facilitates easy interchange of the Si microchannel, allowing one to fabricate channels with dimensions specific to the desired power.

3.3.4. 3 mm and 5 mm wide microchannels

While these arrays have five times the effective surface area of a single channel, they take up more physical space, require a larger electrode (thus using more electrode material than a single channel) and require a larger clamp to accommodate the increased width of the Si array. The arrays also require greater pumping speeds in order to alleviate the problem of air bubbles disrupting the laminar flow of the arrayed system and to allow total filling of all the channels. In order to alleviate this problem, microchannels which were 3 mm in width were fabricated. These do not require a larger clamp (than that of a 1 mm wide channel) nor require more electrode material, as well as do not seem to require a much faster pumping speed than for the single lmm wide microchannels. The effective surface area available to generate power was about 1.2 cm^2 (that is, smaller than three times that of a single 1 mm wide microchannel) due to the fact that the tapered flow boundary was fabricated to be slightly longer than the previous 1 mm wide channels. This meant that the performance of the 3 mm wide channel should be approximately twice that of a single channel in terms of power generation. We tested the 3 mm wide, 380 μm thick, Si microchannel with a pumping speed of 2 ml min^{-1}. Table 1 shows the results for this channel. The power obtained was 160 μW, which demonstrates that indeed, the 3 mm wide channel gave results that were approximately twice the maximum power obtained from our best single 1 mm wide channels.

It is important to maximize power output in a minimum amount of space. For this reason, microchannels which were 5 mm wide, 250 μm thick, and 5 cm in length were also fabricated in order to afford the same advantages as mentioned above for the 3 mm wide channel. This microchannel was expected to produce power comparable to that produced from the 5-microchannel array. Unlike for the 3 mm wide channels, a problem with these 5 mm wide channel electrodes was encountered. While the Kapton® electrodes could be cut to any size, they had a tendency to drape across, and into, the 5 mm wide channel, thus interrupting laminar flow. In order to circumvent this problem, Si was used as a substrate for the platinum electrodes. The Si was etched to produce fluid inlet and outlet holes in order for the fuel and oxidant to be injected into the Si microchannel and between the two electrodes. A thin film composed of 50 nm of Ta and 50 nm of Pt was evaporated onto the Si surface to serve as the electrode. These electrodes were then clamped on either side of the 5 mm wide channel using the same clamping device employed previously. Table 1 shows the results for this device and, as for the 3 mm wide microchannel case, the power output for the 5 mm wide channels scaled linearly with the single 1 mm wide channels. It also performed just as well as the 5-microchannel arrays, producing 325 μW from a single device.

3.3.5. Stacked cells

As indicated above, one of the goals of constructing a PM^2FC was to generate the maximum amount of power in a minimum amount of space. Achieving this objective required the stacking of multiple devices. We have already demonstrated that power maximization in a single channel can be achieved by varying the channel width, as well as constructing an array of five microchannels. The last aspect of our planar design that was tested was the ability to stack our microchannels. In order to demonstrate this aspect, 1 mm stackable channels were fabricated. Two single 1 mm wide microchannels were placed one on top of the other and Kapton® electrodes were placed in between each one in order to form

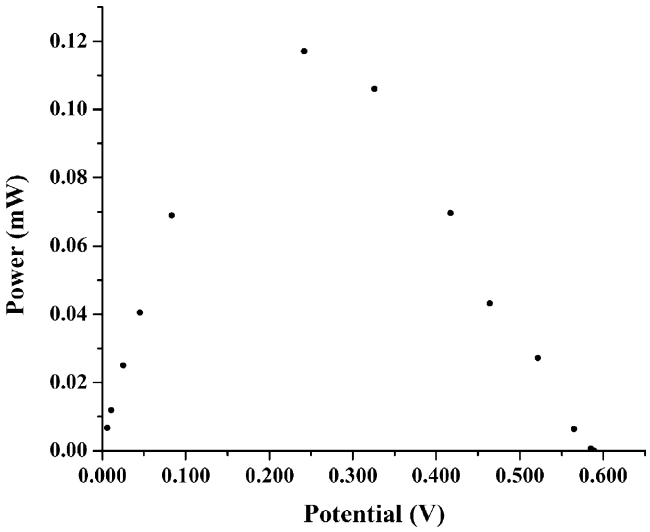

Fig. 10. Power output for a stack of two 1 mm wide channels, 380 μm thick. Kapton® electrodes with 50 nm of Ta and 50 nm of Pt were used. Fuel was 0.5 M formic acid in 0.1 M H_2SO_4 bubbled with N_2, oxidizer was 0.1 M H_2SO_4 aerated with O_2, flow rate = 1.5 ml min^{-1}.

a micro-fuel cell stack. The entire system was pumped with a single syringe pump and a clamp with the same dimensions as that used for 1 mm wide channels was employed. Fig. 10 below shows the power output results for a stack of two 1 mm wide, 380 μm thick microchannels. The stack of two single 1 mm wide microchannels produced 116 μW, which can be compared to the nearly 45 μW produced from a single 1 mm wide microchannel. The two-channel stack produced twice the power of a single channel without increasing the physical volume of the PM^2FC. These results demonstrate that planar microchannels can be stacked in order to increase power generation. This is a great advantage in terms of manufacturing high-powered compact devices, which can only be achieved with such a planar design. The stacking will be investigated further in terms of stacking multiple channels, wider channels, as well as arrays.

4. Conclusions

This PM^2FC design has a number of advantages over other micro-fuel cells. It maximizes power production due to the large electrode areas that are available to come into contact with the fuel and oxidizer stream and is a versatile platform for the rapid testing of fuel systems, electrodes, and microchannel designs. The design also allows microchannels to be stacked in order to increase power production from a single device. This design demonstrated that under laminar flow conditions, a PEM is not needed in order to produce a micro-fuel cell that generates power. With no PEM, the fabrication of the micro-fuel cell itself becomes facile, less expensive than current designs, as well as more easily optimized in terms of electrode development.

With electrode geometric areas of 0.5–2.5 cm^2, we have obtained 0.045–0.4 mW depending on the microchannel dimensions. The ability to fabricate microchannels of varying widths, as well as stack microchannels, using this planar design allows power production to be enhanced without greatly increasing the physical volume of the micro-fuel cell itself. Also, major changes to the PM^2FC platform are not needed between different microchannel experiments because both fuel and oxidizer are injected into the microchannel from the top and the platform can support a number of microchannel geometries. Maximum power in a minimum volume is one of the important goals when designing a micro-fuel cell and this design is conducive to achieving that goal.

The formic acid fuel cell system, employed here as a test system, has shown comparable performance to that reported previously for micro-, and macro-, fuel cell systems. The power production is limited by the kinetics of the formic acid oxidation, as well as the concentration of the O_2 at the cathode. The open circuit potential is largely limited by the overpotential for oxygen reduction. By modifying the anode electrode surface with adsorbed Bi adatoms, and subsequently catalyzing the formic acid oxidation, one can increase the open circuit potential of the fuel cell.

Future work will include studies of H_2/O_2 fuel cells in acidic and basic electrolyte in order to compare their performance to macro-scale fuel cells. Incorporation of Pt and PtRu nanoparticles, as well as intermetallic micro-, and nanoparticles such as PtBi and PtPb will also be investigated as anode catalysts, which will facilitate further investigation of formic acid, as well as other fuel systems, such as methanol and ethanol. The versatility of this planar platform will allow rapid analysis and characterization of the systems with various catalysts at different flow rates, microchannel thicknesses, and widths. The microchannels will continue to be tested and their length, width, and thickness will be optimized to give the maximum power density using a minimum physical area. Alternative substrates for the microchannels will also be investigated in the future including polyimides, such as Kapton®, or poly(dimethylsiloxane) (PDMS). Both of these materials will facilitate the development of flexible planar devices that are very thin. There is a great emphasis on movement towards using polymers for micro-devices because of their ease of fabrication, cost efficiency, and physical flexibility [28–30]. The device design proposed here is conducive to this type of fabrication and future work will be driven toward the development of a flexible planar micro-fuel cell, which in turn could have a wide range of applications in biology, micro-materials design, and small electronic device power systems.

Acknowledgements

This research was generously funded by ARO (DAAD19-03-C-0100) and NSF (ACT-0346377). This work was performed in part at the Cornell NanoScale Facility (a mem-

ber of the National Nanotechnology Infrastructure Network) which is supported by the National Science Foundation under Grant ECS-0335765, its users, Cornell University and Industrial Affiliates.

References

[1] For example, www.fuelcellstoday.com.
[2] J.S. Wainright, R.F. Savinell, C.C. Liu, M. Litt, Electrochim. Acta 48 (2003) 2869–2877.
[3] S.C. Kelley, G.A. Deluga, W.H. Smyrl, Electrochem. Solid-State Lett. 3 (2000) 407–409.
[4] J. Yu, P. Cheng, Z. Ma, B. Yi, Electrochim. Acta 48 (2003) 1537–1541.
[5] S.J. Lee, A. Chang-Chien, S.W. Cha, R. O'Hayre, Y.I. Park, Y. Saito, F.B. Prinz, J. Power Sources 112 (2002) 410–418.
[6] H.L. Maynard, J.P. Meyers, J. Vac. Sci. Technol. B 20 (2002) 1287–1297.
[7] J. Yu, P. Cheng, Z. Ma, B. Yi, J. Power Sources 124 (2003) 40–46.
[8] G.T.R. Palmore, H. Bertschy, S.H. Bergens, G.M. Whitesides, J. Electroanal. Chem. 443 (1998) 155–161.
[9] A.J. Appleby, D.Y.C. Ng, H. Weinstein, J. Appl. Electrochem. 1 (1971) 79–90.
[10] G.T.R. Palmore, H.-H. Kim, J. Electroanal. Chem. 464 (1999) 110–117.
[11] E. Katz, I. Willner, A.B. Kotlyar, J. Electroanal. Chem. 479 (1999) 64–68.
[12] N. Mano, F. Mao, A. Heller, J. Am. Chem. Soc. 124 (2002) 12962–12963.
[13] N. Mano, F. Mao, A. Heller, J. Am. Chem. Soc. 125 (2003) 6588–6594.
[14] N. Mano, F. Mao, W. Shin, T. Chen, A. Heller, Chem. Commun. (2003) 518–519.
[15] A.E. Kamholz, B.H. Weigl, B.A. Finlayson, P. Yager, Anal. Chem. 71 (1999) 5340–5347.
[16] P.J.A. Kenis, R.F. Ismagilov, G.M. Whitesides, Science 285 (1999) 83–85.
[17] P.J.A. Kenis, R.F. Ismagilov, S. Takayama, G.M. Whitesides, Acc. Chem. Res. 53 (2000) 841–847.
[18] R.F. Ismagilov, A.D. Stroock, P.J.A. Kenis, G. Whitesides, H.A. Stone, Appl. Phys. Lett. 76 (2000) 2376–2378.
[19] R. Ferrigno, A.D. Stroock, T.D. Clark, M. Mayer, G.M. Whitesides, J. Am. Chem. Soc. 124 (2002) 12930–12931.
[20] E.R. Choban, P. Waszczuk, L.J. Markoski, A. Wieckowski, P.J.A. Kenis, Power Sources Proc. 40 (2003) 317–320.
[21] E.R. Choban, L.J. Markoski, A. Wieckowski, P.J.A. Kenis, J. Power Sources 128 (2004) 54–60.
[22] S.P.E. Smith, H.D. Abruña, J. Phys. Chem. B 102 (1998) 3506–3511.
[23] C. Rice, S. Ha, R.I. Masel, P. Waszczuk, A. Wieckowski, T. Barnard, J. Power Sources 111 (2002) 83–89.
[24] M. Weber, J.-T. Wang, S. Wastnus, R.F. Savinell, J. Electrochem. Soc. 143 (1996) L158–L160.
[25] G.M. Bommarito, D. Acevedo, H.D. Abruña, J. Phys. Chem. 96 (1992) 3416–3419.
[26] V. Climent, E. Herrero, J.M. Feliu, Electrochim. Acta 44 (1998) 1403–1414.
[27] A. Fernandez-Vega, J.M. Feliu, A. Aldaz, J. Clavilier, J. Electroanal. Chem. 305 (1991) 229–240.
[28] Y. Xia, G.M. Whitesides, Annu. Rev. Mater. Sci. 28 (1998) 153–184.
[29] H. Schmid, H. Wolf, R. Allenspach, H. Riel, S. Karg, B. Michel, E. Delamarche, Adv. Fund. Mater. 13 (2003) 145–153.
[30] J.C. McDonald, G.M. Whitesides, Acc. Chem. Res. 35 (2002) 491–499.